

# 000 001 002 003 004 005 006 007 008 009 010 011 012 013 014 015 016 017 018 019 020 021 022 023 024 025 026 027 028 029 030 031 032 033 034 035 036 037 038 039 040 041 042 043 044 045 046 047 048 049 050 051 052 053 VISUAL PROGRAMMABILITY: A GUIDE FOR CODE-AS-THOUGHT IN CHART UNDERSTANDING

Anonymous authors

Paper under double-blind review

## ABSTRACT

Chart understanding presents a critical test to the reasoning capabilities of Vision-Language Models (VLMs). Prior approaches face critical limitations: some rely on external tools, making them brittle and constrained by a predefined toolkit, while others fine-tune specialist models that often adopt a single reasoning strategy, such as text-based chain-of-thought (CoT). The intermediate steps of text-based reasoning are difficult to verify, which complicates the use of reinforcement-learning signals that reward factual accuracy. To address this, we propose a Code-as-Thought (CaT) approach to represent the visual information of a chart in a verifiable, symbolic format. Our key insight is that this strategy must be adaptive: a fixed, code-only implementation consistently fails on complex charts where symbolic representation is unsuitable. This finding leads us to introduce **Visual Programmability**: a learnable property that determines if a chart-question pair is better solved with code or direct visual analysis. We implement this concept in an **adaptive** framework where a VLM learns to choose between the CaT pathway and a direct visual reasoning pathway. The selection policy of the model is trained with reinforcement learning using a novel dual-reward system. This system combines a data-accuracy reward to ground the model in facts and prevent numerical hallucination, with a decision reward that teaches the model when to use each strategy, preventing it from defaulting to a single reasoning mode. Experiments demonstrate strong and robust performance across diverse chart-understanding benchmarks. Our work shows that VLMs can be taught not only *to* reason but also *how* to reason, dynamically selecting the optimal reasoning pathway for each task.

## 1 INTRODUCTION

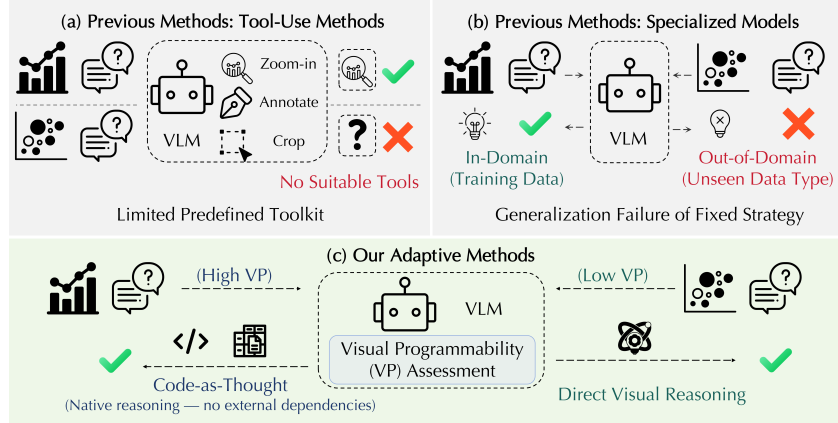


**Figure 1:** Adaptive Reasoning vs. Fixed Strategies for Chart Understanding. Prevailing approaches are limited by their rigid strategies. (a) Tool-Use Models are constrained by a predefined toolkit and fail on novel tasks. (b) Specialized Models employ a single reasoning pattern (e.g., text-only or code-only), which limits their generalization. In contrast, our (c) Adaptive Framework first assesses a task’s Visual Programmability. It then dynamically selects the precise Code-as-Thought pathway for programmable tasks or the robust **Direct Visual Reasoning** pathway for complex ones, achieving superior performance across all chart types.

054 The capabilities of Vision-Language Models (VLMs), built upon powerful Large Language Mod-  
 055 els Brown et al. (2020); Touvron et al. (2023), have rapidly advanced multimodal understanding  
 056 (e.g., Radford et al. (2021); Liu et al. (2023); Achiam et al. (2023); Comanici et al. (2025); Bai et al.  
 057 (2025)). Among the many applications, chart understanding stands out as a critical benchmark Huang  
 058 et al. (2024), testing an AI’s ability to connect low-level visual perception Lee et al. (2023) with  
 059 high-level logical inference. Despite significant progress with specialized models Cheng et al. (2023);  
 060 Masry et al. (2023); Meng et al. (2024), a fundamental generalization problem remains: even state-  
 061 of-the-art VLMs show a stark performance decline on the complex, “in-the-wild” charts found in  
 062 real-world contexts Islam et al. (2024); Wang et al. (2024).

063 Prevailing efforts to overcome this generalization challenge have largely followed two dominant  
 064 strategies, each with distinct drawbacks. The first approach treats the VLM as a controller for external  
 065 tools and APIs Huang et al. (2025); Gupta & Kembhavi (2023); Surís et al. (2023) (see Figure 1a).  
 066 While powerful, their reliance on a predefined toolkit makes them brittle when encountering charts  
 067 that require capabilities beyond their predefined functions Schick et al. (2023); Yao et al. (2023b);  
 068 Patil et al. (2024); Parisi et al. (2022). The second strategy involves fine-tuning specialized models on  
 069 chart-specific data Cheng et al. (2023); Masry et al. (2023); Meng et al. (2024) (see Figure 1b). These  
 070 models typically rely on a *monolithic reasoning pattern*—that is, they exclusively use a single mode  
 071 of thought, such as text-based Chain-of-Thought or code-based reasoning. This lack of flexibility  
 072 hinders their ability to generalize to out-of-distribution (OOD) visualizations, as no single reasoning  
 073 style is optimal for all chart types Wang et al. (2024); Xu et al. (2023).

074 The limitations of predefined toolkits highlight the appeal of a more universal and flexible tool: code.  
 075 Unlike a fixed API, code can be dynamically generated to create novel tools tailored to the specific  
 076 visual complexities of any chart, a concept explored in recent agentic vision systems Zhao et al.  
 077 (2025a). However, the shared failure of rigid approaches motivates our core insight: the optimal  
 078 reasoning strategy depends on the task itself. Some charts are easily broken down into programmable  
 079 elements Dai et al. (2024), while others require a holistic visual analysis that code cannot capture.  
 080 This requires moving beyond refining a single reasoning chain Wei et al. (2022) to mastering strategy  
 081 selection—a shift that reflects a broader trend in AI towards deliberate problem-solving Wang et al.  
 082 (2022); Shinn et al. (2023); Yao et al. (2023a) and adaptive computation Graves (2016). This principle  
 083 is also central to the design of frontier models like GPT-5 OpenAI (2025), which aim to integrate  
 similar adaptive capabilities.

084 To address these challenges, we propose the concept of **Visual Programmability**: a learnable,  
 085 task-dependent property that indicates whether a given chart-question pair is best solved through pro-  
 086 grammatic reasoning or direct visual analysis. We implement this concept in an adaptive framework  
 087 that enables a VLM to autonomously choose its reasoning pathway. The model’s decision-making  
 088 policy is trained via reinforcement learning (RL)—specifically, using the Group Relative Policy  
 089 Optimization (GRPO) algorithm—guided by a novel **dual-reward system**. This system is carefully  
 090 designed to foster adaptive behavior: a data-accuracy reward ensures the generated code is factually  
 091 grounded to the chart’s content, thereby preventing numerical hallucination. In parallel, a dedicated  
 092 decision reward explicitly teaches the model the boundaries of programmability, preventing the policy  
 093 from collapsing into a single, suboptimal mode.

094 Experiments with Qwen2.5-VL Bai et al. (2025) across diverse benchmarks validate our approach.  
 095 The adaptive model outperforms pure-vision and fixed code baselines by selecting its strategy—using  
 096 code when advantageous (**>60%**) and avoiding it when harmful (**<10%**). Ablations confirm that the  
 097 dual-reward design prevents mode collapse and promotes strategic diversity. Our contributions are  
 098 threefold:

- 100 • We introduce **Visual Programmability**, a novel concept to determine if a chart task is  
 101 suitable for code-based reasoning, serving as the foundation for adaptive strategy selection.
- 102 • Building on this concept, we develop an **adaptive framework** that learns to choose the  
 103 optimal reasoning path (code or vision). This framework is trained with a specialized  
 104 dual-reward RL system that promotes both factual accuracy and strategic flexibility.
- 106 • Our adaptive model demonstrates **outstanding performance and generalization**, consist-  
 107 ently outperforming rigid strategies across diverse benchmarks by intelligently switching  
 between reasoning modes.

108 **2 RELATED WORK**  
 109

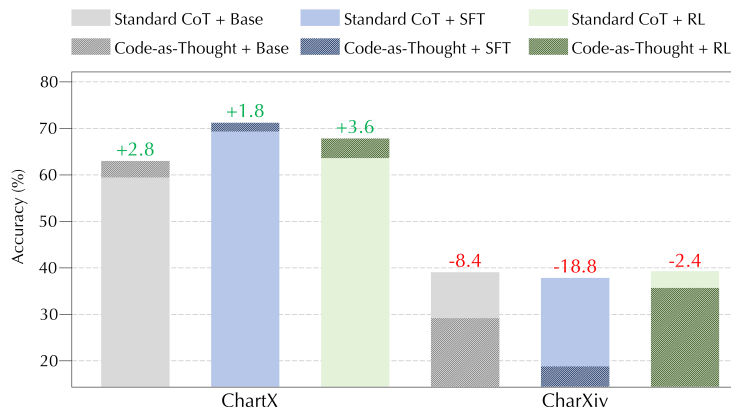
110 **Programmatic Reasoning and Its Limits.** The field of chart understanding has seen a shift towards  
 111 programmatic reasoning. This includes VLMs acting as controllers for external tools Gao et al.  
 112 (2023); Schick et al. (2023); Surís et al. (2023) and models that generate code as a form of symbolic  
 113 thought Subramanian et al. (2023); Chen et al. (2023). While specialized models achieved high  
 114 scores on earlier benchmarks Cheng et al. (2023); Masry et al. (2023), their success was often  
 115 misleading. They tended to learn benchmark-specific shortcuts, a weakness exposed by a new wave  
 116 of diverse and complex benchmarks Xia et al. (2024); Wang et al. (2024); Xu et al. (2023), where  
 117 even state-of-the-art models show a significant performance drop Islam et al. (2024); Huang et al.  
 118 (2024). We argue that this generalization gap stems not from a lack of model capability, but from  
 119 *strategic rigidity*. Despite variations in approach—from Mixture-of-Experts Xu et al. (2024) to visual  
 120 grounding techniques Ni et al. (2025); Huang et al. (2025)—existing methods adhere to a fixed  
 121 reasoning pattern. Our work departs from this by reframing the challenge: instead of augmenting  
 122 VLMs with external tools, we teach them to recognize *when* to deploy their own code-like reasoning,  
 123 shifting the focus from tool use to strategic selection.  
 124

125 **Adaptive Learning for Strategic Reasoning.** Our framework builds on the idea of adaptive  
 126 computation, where a system alters its strategy based on the input Bengio et al. (2015); Kahneman  
 127 (2011). In AI, this is often implemented through methods like dynamic routing or Mixture-of-Experts  
 128 layers, which adapt *how* a model performs its computation Sabour et al. (2017); Jiang et al. (2024).  
 129 We apply this concept at a higher level: we teach a model to decide *what* reasoning process to use, a  
 130 skill we call *strategic cognition*. Reinforcement learning (RL) is well-suited for learning such a policy  
 131 from outcome-based feedback, a technique proven effective for tasks with verifiable answers Meng  
 132 et al. (2025); Su et al. (2025); Lightman et al. (2023). However, a simple accuracy reward can cause  
 133 the model to always default to a single, safe strategy—a problem known as *mode collapse*. Our key  
 134 contribution is a **dual-reward system** that combines an accuracy signal with a dedicated decision  
 135 reward. This design encourages strategic diversity, teaching the model not just to solve the task, but  
 136 how to choose the right reasoning tool for the job.  
 137

138 **3 EXPLORING CODE-AS-THOUGHT AS A UNIVERSAL STRATEGY**  
 139

140 The limitations of the fixed strategies discussed previously motivate us to explore whether a more  
 141 powerful, formal paradigm could serve as a universal solution for chart understanding. This line of  
 142 inquiry leads us to investigate Code-as-Thought (CaT) and to pose a foundational question:  
 143

144 *Is Code-as-Thought a "silver bullet" for chart understanding?*  
 145



147 **Figure 2: Performance of Fixed Strategies Highlights a Critical Trade-off.** While the Code-as-Thought  
 148 (CaT) strategy excels on structured charts (ChartX), its performance collapses on complex, 'in-the-wild'  
 149 charts (CharXiv). All values are accuracy (%).  
 150

151 To answer this, we first investigated the efficacy of a single, fixed CaT strategy. We trained a  
 152 specialist model on structured data and evaluated its generalization across four diverse benchmarks.  
 153

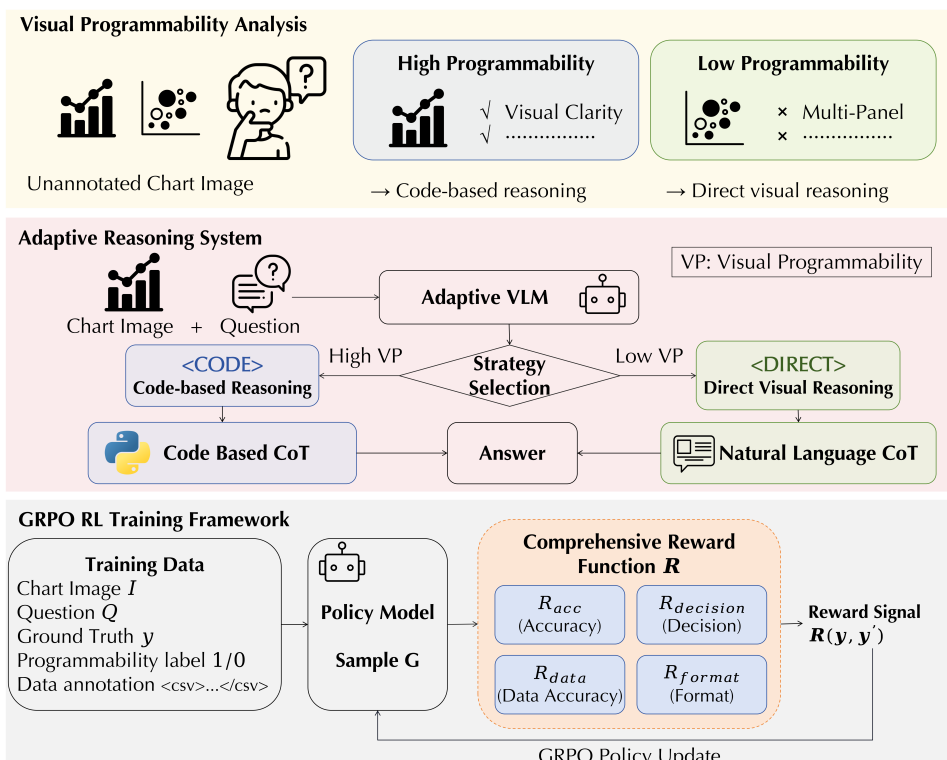
162 We discovered a core limitation that motivates our adaptive framework. Figure 2 visualizes the  
 163 results on two of these benchmarks—the highly structured ChartX and the complex, "in-the-wild"  
 164 CharXiv—which most clearly illustrate the performance trade-offs. A detailed description of the  
 165 setup and full results across all four benchmarks are provided in Appendix A.

166 The results reveal a sharp dichotomy in generalization performance. As shown in Figure 2, the CaT  
 167 specialist (achieving 71.6% with SFT) excels on the structured ChartX data, confirming its power in  
 168 high-programmability scenarios. However, this rigid strategy proves brittle. On the complex charts  
 169 from CharXiv, its accuracy collapses to a mere 18.4%. This failure is often driven by numerical  
 170 hallucination—where the model generates code from a flawed perception of the chart, then reasons  
 171 faithfully from this incorrect foundation. A case of this phenomenon is detailed in Appendix B.

172 Furthermore, we found that enhanced skill and policy optimization are not a panacea. The right side of  
 173 the figure illustrates that even after applying reinforcement learning (RL), the model’s performance on  
 174 CharXiv remains critically low, failing to resolve the core conflict. Results with extensive pre-training  
 175 (CPT+RL) exhibit the same trend and are provided in Appendix A. The conclusion is clear: the  
 176 issue is not the model’s competence (how well it codes) but determining the strategy’s applicability  
 177 (whether it *should* code at all). These experiments confirm the potential of Code-as-Thought but  
 178 reveal that the optimal strategy is task-dependent, motivating our core thesis: an intelligent system  
 179 must learn *when* to use its tools, not just how.

## 181 4 ADAPTIVE CODE-BASED REASONING FRAMEWORK

182 Our framework enables a Vision-Language Model (VLM) to dynamically select the optimal reasoning  
 183 strategy for a given chart. As illustrated in Figure 3, it consists of three core parts: an adaptive  
 184 inference system, a training process based on reinforcement learning, and the underlying concept of  
 185 Visual Programmability that guides the model’s learning.



212 **Figure 3:** Overview of our adaptive reasoning framework. **(Top)** We introduce the concept of Visual Programmability  
 213 and use it to guide data annotation. **(Middle)** At inference, our adaptive VLM selects a reasoning pathway  
 214 based on the perceived Visual Programmability (VP) of the task. **(Bottom)** The model’s selection policy is  
 215 trained using reinforcement learning with a multi-component reward function and the GRPO algorithm.

216  
217

## 4.1 VISUAL PROGRAMMABILITY: UNDERSTANDING THE BOUNDARIES OF CODE

218  
219  
220  
221  
222  
223

Not all charts are equally well-suited to analysis using Code-as-Thought. To address this, we introduce the concept of **Visual Programmability**: a learnable, task-dependent property that serves as the foundation for our adaptive reasoning system. It determines whether a chart-question pair can be faithfully reasoned using code. This property is not a binary yes-or-no question; rather, it represents a range of suitability influenced by a chart’s structural clarity, its visual complexity, and the query itself. Figure 4 provides several cases that illustrate this concept.

224  
225  
226  
227  
228  
229  
230  
231

**High vs. Low Programmability.** The suitability of code-based reasoning varies widely. Some charts exhibit high programmability. These are typically standard bar, line, or scatter plots with clean layouts, where the underlying data can be programmatically extracted with high fidelity. Figure 4 (a) shows a clear example: a standard line chart with explicitly marked data points, making it ideal for precise computational analysis. In contrast, other charts have low programmability. As seen in Figure 4 (b), these often include complex scientific visualizations where meaning is conveyed through holistic patterns, such as data contours and distributions. For these charts, essential information is often lost or distorted during symbolic translation.

232  
233  
234  
235  
236  
237  
238  
239

**The Critical Role of Task Dependency.** Crucially, Visual Programmability is not an intrinsic chart property alone; it is fundamentally dependent on the user’s query. This is demonstrated by the case in Figure 4 (c). For a simple counting task like, “*How many distinct data series are plotted?*”, the chart has **high programmability**, as the task only requires identifying discrete visual elements. However, for a value-extraction task like, “*What is the approximate value of the orange line ( $h/a = 1000$ ) when  $d = 7$ ?*”, the same chart exhibits **low programmability**. The logarithmic scale makes precise data extraction extremely difficult and error-prone. In this scenario, a Code-as-Thought approach would likely yield a confidently incorrect answer, making direct visual reasoning a more reliable strategy.

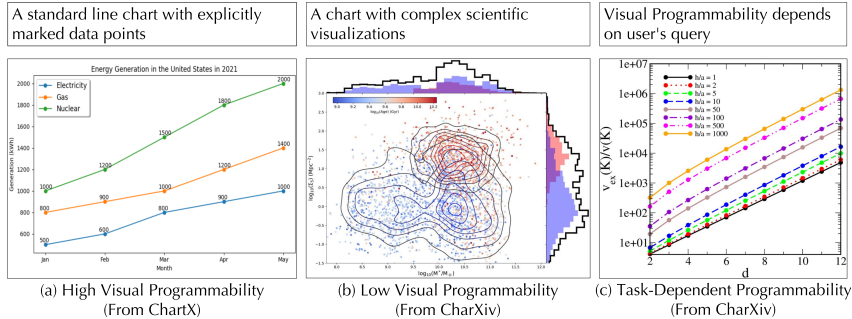
240  
241  
242  
243  
244  
245  
246  
247  
248  
249  
250  
251

Figure 4: Cases of Visual Programmability for different charts and tasks.

252  
253  
254  
255  
256

This dependency on both the chart and the question necessitates a dynamic reasoning system. An intelligent agent cannot rely on a fixed strategy; it must learn to assess Visual Programmability to select the most appropriate reasoning path. To enable this, we developed a framework to annotate data for this property, providing the signal for learning this adaptive skill (see Appendix C).

257

## 4.2 ADAPTIVE REASONING MECHANISM

258  
259  
260  
261  
262

We formulate the chart-understanding task as a policy learning problem. Given a chart image  $\mathbf{I}$  and a question  $\mathbf{Q}$ , our model learns a policy  $\pi_\theta$  that generates a response  $\mathbf{y}$ . This process is explicitly factorized to first select a strategy token  $s \in \{\langle \text{CODE} \rangle, \langle \text{DIRECT} \rangle\}$ , then generate the corresponding reasoning and answer:

$$P(\mathbf{y}|\mathbf{I}, \mathbf{Q}) = P(s|\mathbf{I}, \mathbf{Q}) \cdot P(\mathbf{y}|\mathbf{I}, \mathbf{Q}, s). \quad (1)$$

263  
264  
265  
266  
267

This factorization is realized by building upon powerful base models (Qwen2.5-VL) and teaching them to first commit to a strategy by generating a special token, which then dictates the subsequent generation path:

268  
269

**Code-based Path ( $\langle \text{CODE} \rangle$ ):** The model generates a Code-as-Thought (CaT) pathway. It writes code to parse the chart into a structured format (e.g., a DataFrame) and then performs computations to find the answer. This path is ideal for charts with high Visual Programmability.

270 **Direct Path (<DIRECT>):** The model generates a natural language CoT, performing reasoning based  
 271 on its holistic visual perception. This path is essential for charts with low Visual Programmability  
 272 where symbolic decomposition would lose critical information.

273 For automated evaluation, the final answer from both paths must be enclosed in `\boxed{ }.`

### 275 4.3 TRAINING VIA REINFORCEMENT LEARNING

277 The crucial challenge is the absence of ground-truth labels for strategy selection. We overcome this  
 278 by formulating the training as a reinforcement learning problem, allowing the model to learn the  
 279 optimal policy from outcome-based reward signals.

#### 281 4.3.1 GRPO POLICY UPDATE

283 We optimize the policy with Group Relative Policy Optimization (GRPO). For each input, we sample  
 284 a group of  $G$  rollouts from  $\pi_{\text{old}}$ , score them with our reward, compute group-normalized advantages,  
 285 and apply a clipped-ratio update. We follow a KL-free configuration by setting  $\beta=0$ . The full  
 286 objective, notation, and update details are provided in Appendix G.

#### 287 4.3.2 COMPREHENSIVE REWARD FUNCTION

289 A naive reward function focused solely on answer accuracy would be insufficient and could lead  
 290 to *mode collapse*—where the model defaults to a single, suboptimal strategy. To prevent this and  
 291 guide the model toward true adaptive behavior, we designed a comprehensive reward function  $R$  as a  
 292 weighted sum of four specialized components:

$$293 R = w_{\text{acc}} r_{\text{acc}} + w_{\text{decision}} r_{\text{decision}} + w_{\text{data}} r_{\text{data}} + w_{\text{format}} r_{\text{format}}. \quad (2)$$

294 The components are:

296 **Accuracy Reward ( $r_{\text{acc}}$ ):** The primary reward, providing a binary signal (1.0 or 0.0) based on the  
 297 correctness of the final answer.

298 **Decision Reward ( $r_{\text{decision}}$ ):** Our key innovation to prevent mode collapse. This reward explicitly  
 299 incentivizes selecting the correct strategy based on the chart's pre-annotated Visual Programmability.  
 300 It gives a full reward for a correct answer via the correct strategy, a partial reward for a wrong answer  
 301 but using the correct strategy (to encourage exploration), and zero reward for using the wrong strategy.  
 302 This component is essential for teaching the model to learn the decision boundary.

$DF_{gt}$			① Column Match (Fuzzy Match)			② Raw Count		
Date	Total Sales	Category	$DF_{gt}$	Date	Total Sales	$DF_{gt}$	3	
2024-01-01	1000	A	$DF_{pred}$	Date	sale total	$DF_{pred}$	3	
2024-01-02	1500	B		√	×		√	
2024-01-03	1300	A		√	√		√	
			$r_{\text{col}} = 2/3 = 0.6667$			$r_{\text{raw}} = 1.0$		
$DF_{pred}$			③ Value Accuracy (Compare Matched Columns)					
Date	sale total	category	$DF_{gt}$	$DF_{pred}$		$DF_{gt}$	$DF_{pred}$	
2024-01-01	1000	A	Date	Date		Category	category	
2024-01-02	1500	B	√	√	√	A	A	√
2024-01-03	1800	C	√	√	√	B	B	√
			$r_{\text{values}} = 5/6 = 0.8333$					
$r_{\text{data}} = \alpha \cdot r_{\text{col}} + \beta \cdot r_{\text{raw}} + \theta \cdot r_{\text{values}}$								

313 **Figure 5:** Illustration of the Data Accuracy Reward calculation.

314 **Data Accuracy Reward ( $r_{\text{data}}$ ):** Applied *only* to the <CODE> path, this reward tackles the issue  
 315 of code "hallucination." It programmatically compares the DataFrame generated by the model's  
 316 code to a ground-truth data table, evaluating the fidelity of the extracted data. This ensures the  
 317 model generates code that is not just syntactically valid, but semantically faithful to the chart. The  
 318 calculation process is visualized in Figure 5.

319 **Format Reward ( $r_{\text{format}}$ ):** A small reward to enforce correct output structure (i.e., using `\boxed{ }`),  
 320 ensuring reliable parsing.

322 This multi-faceted reward design creates a nuanced optimization landscape that simultaneously  
 323 pushes the model toward accuracy and strategic intelligence. The detailed implementation of the  
 Data Accuracy Reward is provided in Appendix E.

324 

## 5 EXPERIMENTS

325 

### 5.1 EXPERIMENTAL SETUP

328 We train on ChartMimic Yang et al. (2024) augmented with automatically generated QA pairs  
 329 (Gemini-2.5-Flash; prompts in Appendix F) to cover both programmable and non-programmable  
 330 chart-question pairs. We evaluate on four benchmarks spanning the Visual Programmability spectrum:  
 331 ChartX Xia et al. (2024), ChartBench (NQA) Xu et al. (2023), ChartQA Masry et al. (2022), and  
 332 CharXiv Wang et al. (2024). Our base is Qwen2.5-VL-7B trained with GRPO (EasyR1 Zheng et al.  
 333 (2025)) under the dual-reward design in Eq. 2. Full dataset composition, sampling protocol, metric  
 334 definitions, and hyperparameters are detailed in Appendix D.

335 

### 5.2 COMPARISON WITH FIXED-STRATEGY BASELINES

337 **Table 1:** Comparison with fixed-strategy baselines on four benchmarks. Our adaptive RL model achieves the  
 338 highest average accuracy by dynamically selecting its reasoning strategy. All values are accuracy (%).

Model Type	Reasoning Strategy	ChartX	ChartBench	ChartQA	CharXiv	Average
Base Models (No RL)	Standard CoT	59.2	50.1	84.9	38.4	58.2
	Code CoT (Fixed)	59.8	53.4	79.4	28.8	55.4
	Adaptive	57.8	51.4	84.4	22.8	54.1
RL Models	Standard CoT	61.5	52.8	86.6	43.8	61.2
	Code CoT (Fixed)	64.0	54.0	<b>86.7</b>	41.9	61.7
	<b>Adaptive (Ours)</b>	<b>65.6</b>	<b>54.8</b>	86.4	<b>44.3</b>	<b>62.8</b>

347 As shown in Table 1, our adaptive framework achieves the highest average accuracy (**62.8%**), outper-  
 348 forming all fixed-strategy baselines. This advantage stems from its learned ability to dynamically  
 349 select the optimal reasoning path.

350 Table 2 reveals this strategic behavior. On high-programmability benchmarks like ChartX and  
 351 ChartBench, our model favors the code-based path (**76.0%** and **66.6%** usage) to leverage its precision.  
 352 On the complex CharXiv benchmark, it astutely reduces code usage to just **10.1%**, avoiding the  
 353 pitfalls of a rigid code-only approach and achieving the highest accuracy (**44.3%**). The results on  
 354 ChartQA further suggest that our Data Accuracy Reward improves not only *when* the model uses  
 355 code, but also *how reliably* it does so.

356 Qualitative examples (see Appendix I) further highlight this strategic intelligence: our model correctly  
 357 selects the <CODE> path for precise calculations on structured charts and the <DIRECT> path for  
 358 complex plots, successfully navigating scenarios where fixed-strategy baselines fail.

360 **Table 2:** Code usage percentage across benchmarks for our adaptive model versus fixed strategies. The model  
 361 learns to apply code frequently on high-programmability charts and sparingly on low-programmability ones. All  
 362 values are percentages (%).

Model Type	Reasoning Strategy	ChartX	ChartBench	ChartQA	CharXiv
Base Models (No RL)	Standard CoT	0.0	0.0	0.0	0.0
	Code CoT (Fixed)	98.9	100.0	98.3	99.5
	Adaptive	99.7	99.6	98.8	92.9
RL Models	Standard CoT	0.0	0.0	0.0	0.0
	Code CoT (Fixed)	100.0	100.0	100.0	100.0
	<b>Adaptive (Ours)</b>	<b>76.0</b>	<b>66.6</b>	<b>98.3</b>	<b>10.1</b>

371 

### 5.3 COMPARISON WITH STATE-OF-THE-ART MODELS

372 To contextualize our results, we compare our adaptive framework against several state-of-the-art  
 373 (SOTA) models. All models, unless noted, were evaluated under our stringent protocol to ensure a  
 374 fair comparison. As shown in Table 3, our model achieves the highest average accuracy (**62.8%**),  
 375 significantly outperforming other SOTA models. This performance gap, especially on diverse  
 376 benchmarks like ChartX and CharXiv, underscores the advantage of our adaptive reasoning approach.

378 **Table 3:** Comparison with state-of-the-art models on four key generalization benchmarks. Our model demon-  
 379 strates outstanding performance, achieving the highest average accuracy. All values are percentages (%).

Model	Parameters	ChartX	ChartBench	ChartQA	CharXiv	Average
ChartVLM-Large Xia et al. (2024)	8.3B	35.0	28.8	66.7	14.7	36.3
ChartGemma Masry et al. (2024)	3B	28.7	27.5	69.0	20.3	36.4
ChartMoE Xu et al. (2024)	8B	33.6	29.5	74.2	28.3	41.4
Orsta-7B Ma et al. (2025)	7B	60.3	52.0	84.6	41.5	59.6
Point-RFT Ni et al. (2025)	7B	-	-	<b>90.04<sup>†</sup></b>	36.02*	-
Thyme-VL Zhang et al. (2025)	7B	-	-	86.1*	-	-
<b>Ours (Adaptive)</b>	<b>7B</b>	<b>65.6</b>	<b>54.8</b>	86.4	<b>44.3</b>	<b>62.8</b>

\*Results are taken directly from the original paper.

<sup>†</sup>In-domain evaluation result taken from the original paper.

#### 391 5.4 ANALYSIS ON DIFFERENT MODEL SCALES

392 Our approach demonstrates strong scalability. On the 32B model (Table 4), our adaptive framework  
 393 achieves the highest average accuracy (61.0%) and top performance on the challenging ChartX and  
 394 CharXiv benchmarks. The results from the 3B model are more nuanced. While the fixed ‘Code  
 395 CoT’ strategy yields the best average performance (56.5%), we hypothesize the adaptive strategy  
 396 is constrained by the smaller model. It is nonetheless striking that after RL, the ‘Standard CoT’  
 397 model’s performance collapses (from 31.9% to 20.4%), whereas both code-based strategies improve  
 398 substantially. This strongly indicates that our structured, code-centric reward system provides a more  
 399 stable and effective learning signal than a simple accuracy reward on free-form text.

401 **Table 4:** Performance comparison on 3B and 32B models. Our adaptive framework scales effectively to larger  
 402 models, achieving the best overall performance on the 32B scale. The best results in each RL-trained category  
 403 are highlighted in **bold**. All values are accuracy (%).

Model Size	Training	Reasoning Strategy	ChartX	ChartBench	ChartQA	CharXiv	Average
3B	Base Model (No RL)	Standard CoT	48.0	39.2	13.8	26.7	31.9
		Code CoT (Fixed)	51.3	42.0	28.0	29.3	37.7
		Adaptive	1.0	0.7	0.3	10.6	3.2
	RL-Trained	Standard CoT	9.3	9.3	41.8	21.3	20.4
		Code CoT (Fixed)	<b>58.5</b>	<b>48.5</b>	<b>82.3</b>	<b>36.7</b>	<b>56.5</b>
		Adaptive (Ours)	55.6	43.5	73.6	33.6	51.6
32B	Base Model (No RL)	Standard CoT	53.7	47.2	83.4	36.3	55.2
		Code CoT (Fixed)	56.3	49.6	84.8	39.9	57.7
		Adaptive	56.6	45.7	84.4	37.7	56.1
	RL-Trained	Standard CoT	54.7	47.9	84.6	35.9	55.8
		Code CoT (Fixed)	59.6	<b>49.5</b>	<b>87.9</b>	44.5	60.4
		Adaptive (Ours)	<b>60.2</b>	48.4	87.7	<b>47.5</b>	<b>61.0</b>

#### 416 5.5 ABLATION STUDIES

##### 418 5.5.1 DISSECTING THE REWARD FUNCTION

420 Tables 5 and 6 show the effect of our reward components. The **Decision Reward** ( $r_{\text{decision}}$ ) prevents  
 421 mode collapse, without which the model defaults to a rigid 0/100% code usage. While  $r_{\text{decision}}$   
 422 teaches *when* to use code, the **Data Accuracy Reward** ( $r_{\text{data}}$ ) teaches *how* to use it well, preventing  
 423 over-caution. Together, they create a balanced policy for optimal performance.

424 **Table 5:** Ablation study on reward components. The full reward function is essential for achieving the highest  
 425 accuracy. All values are accuracy (%).

Reward Configuration	ChartX	ChartBench	ChartQA	CharXiv	Average
$r_{\text{acc}} + r_{\text{format}}$ (Baseline)	62.2	52.2	<b>86.5</b>	43.6	61.1
+ $r_{\text{data}}$ (w/o $r_{\text{decision}}$ )	64.3	53.5	86.4	39.4	60.9
+ $r_{\text{decision}}$ (w/o $r_{\text{data}}$ )	63.6	52.4	86.3	43.3	61.4
<b>Full Reward (Ours)</b>	<b>65.6</b>	<b>54.8</b>	86.4	<b>44.3</b>	<b>62.8</b>

432 **Table 6:** Code usage percentage in the reward ablation study. The decision reward ( $r_{\text{decision}}$ ) is critical for  
 433 preventing mode collapse and enabling adaptive behavior. All values are percentages (%).

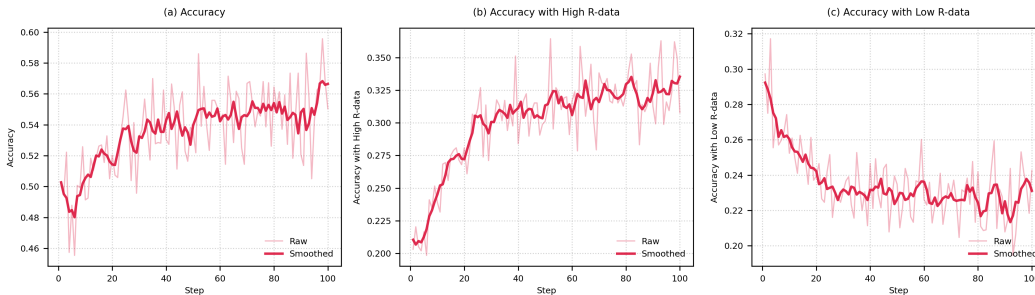
Reward Configuration	ChartX	ChartBench	ChartQA	CharXiv
$r_{\text{acc}} + r_{\text{format}}$ (Baseline)	0.0	0.0	0.0	0.0
+ $r_{\text{data}}$ (w/o $r_{\text{decision}}$ )	100.0	100.0	100.0	100.0
+ $r_{\text{decision}}$ (w/o $r_{\text{data}}$ )	50.4	11.0	87.4	0.7
<b>Full Reward (Ours)</b>	<b>76.0</b>	<b>66.6</b>	<b>98.3</b>	<b>10.1</b>

### 442 5.5.2 THE CRITICAL ROLE OF NUMERICAL FIDELITY

444 This analysis confirms the importance of our data accuracy reward. As shown in Table 7, there is  
 445 a direct and stark correlation between the fidelity of extracted data and the final answer accuracy.  
 446 High-fidelity extraction leads to an impressive **85.6%** accuracy, demonstrating that correct data  
 447 extraction is a prerequisite for successful reasoning on programmable charts. As Figure 6 illustrates,  
 448 our data accuracy reward ( $r_{\text{data}}$ ) grounds the model by teaching it to improve on high-fidelity tasks  
 449 while "unlearning" to guess on low-fidelity ones.

450 **Table 7:** The stark correlation on the ChartX benchmark between the accuracy of extracted numerical data and  
 451 final answer correctness. High-fidelity data extraction is demonstrably a prerequisite for success.

Numerical Accuracy Score ( $r_{\text{data}}$ )	Final Answer Accuracy (%)
< 0.6 (Low Fidelity)	48.4
0.6 - 0.8 (Medium Fidelity)	60.5
> 0.8 (High Fidelity)	<b>85.6</b>



469 **Figure 6:** Training dynamics on ChartX, illustrating the effect of the Data Accuracy Reward ( $r_{\text{data}}$ ). **(Left)**  
 470 Overall task accuracy increases. **(Middle)** Accuracy with high data fidelity ( $r_{\text{data}} > 0.6$ ) rises sharply. **(Right)**  
 471 Accuracy with low data fidelity ( $r_{\text{data}} < 0.6$ ) trends downward, as the model unlearns to guess.

## 475 6 CONCLUSION

477 We challenged the prevailing one-size-fits-all paradigm in visual reasoning. To this end, we introduced  
 478 **Visual Programmability**, a concept that explains why powerful Code-as-Thought (CaT) strategies  
 479 excel on structured charts but fail on complex ones. Building on this insight, we developed an  
 480 adaptive framework trained with a novel dual-reward system. Our model learns to dynamically select  
 481 between the precision of CaT and the robustness of direct visual reasoning, deploying the optimal  
 482 strategy for each task. The key insight from our work is that robust, general-purpose reasoning  
 483 emerges not from a superior monolithic strategy, but from the meta-cognitive skill of knowing one's  
 484 own capabilities and limitations. This work provides a concrete blueprint for building more flexible  
 485 AI systems—systems that don't just follow procedures, but strategically decide how to think. A  
 detailed discussion of limitations, future work, and broader implications is provided in Appendix H.

486 REFERENCES  
487

488 Josh Achiam, Steven Adler, Sandhini Agarwal, Lama Ahmad, Ilge Akkaya, Florencia Leoni Aleman,  
489 Diogo Almeida, Janko Altenschmidt, Sam Altman, Shyamal Anadkat, et al. Gpt-4 technical report.  
490 *arXiv preprint arXiv:2303.08774*, 2023.

491 Shuai Bai, Keqin Chen, Xuejing Liu, Jialin Wang, Wenbin Ge, Sibo Song, Kai Dang, Peng Wang,  
492 Shijie Wang, Jun Tang, et al. Qwen2. 5-vl technical report. *arXiv preprint arXiv:2502.13923*,  
493 2025.

494 Emmanuel Bengio, Pierre-Luc Bacon, Joelle Pineau, and Doina Precup. Conditional computation in  
495 neural networks for faster models. *arXiv preprint arXiv:1511.06297*, 2015.

496 Tom Brown, Benjamin Mann, Nick Ryder, Melanie Subbiah, Jared D Kaplan, Prafulla Dhariwal,  
497 Arvind Neelakantan, Pranav Shyam, Girish Sastry, Amanda Askell, et al. Language models are  
498 few-shot learners. *Advances in neural information processing systems*, 33:1877–1901, 2020.

499 Zhenfang Chen, Rui Sun, Wenjun Liu, Yining Hong, and Chuang Gan. Genome: generative neuro-  
500 symbolic visual reasoning by growing and reusing modules. *arXiv preprint arXiv:2311.04901*,  
501 2023.

502 Zhi-Qi Cheng, Qi Dai, and Alexander G Hauptmann. Chartreader: A unified framework for chart  
503 derendering and comprehension without heuristic rules. In *Proceedings of the IEEE/CVF Interna-  
504 tional Conference on Computer Vision*, pp. 22202–22213, 2023.

505 Gheorghe Comanici, Eric Bieber, Mike Schaeckermann, Ice Pasupat, Noveen Sachdeva, Inderjit  
506 Dhillon, Marcel Blistein, Ori Ram, Dan Zhang, Evan Rosen, et al. Gemini 2.5: Pushing the frontier  
507 with advanced reasoning, multimodality, long context, and next generation agentic capabilities.  
508 *arXiv preprint arXiv:2507.06261*, 2025.

509 Yue Dai, Soyeon Caren Han, and Wei Liu. Msg-chart: Multimodal scene graph for chartqa. In *Pro-  
510 ceedings of the 33rd ACM International Conference on Information and Knowledge Management*,  
511 pp. 3709–3713, 2024.

512 Luyu Gao, Aman Madaan, Shuyan Zhou, Uri Alon, Pengfei Liu, Yiming Yang, Jamie Callan, and  
513 Graham Neubig. Pal: Program-aided language models. In *International Conference on Machine  
514 Learning*, pp. 10764–10799. PMLR, 2023.

515 Alex Graves. Adaptive computation time for recurrent neural networks. *arXiv preprint  
516 arXiv:1603.08983*, 2016.

517 Tanmay Gupta and Aniruddha Kembhavi. Visual programming: Compositional visual reasoning  
518 without training. In *Proceedings of the IEEE/CVF conference on computer vision and pattern  
519 recognition*, pp. 14953–14962, 2023.

520 Kung-Hsiang Huang, Hou Pong Chan, Yi R Fung, Haoyi Qiu, Mingyang Zhou, Shafiq Joty, Shih-Fu  
521 Chang, and Heng Ji. From pixels to insights: A survey on automatic chart understanding in the era  
522 of large foundation models. *IEEE Transactions on Knowledge and Data Engineering*, 2024.

523 Muye Huang, Lingling Zhang, Jie Ma, Han Lai, Fangzhi Xu, Yifei Li, Wenjun Wu, Yaqiang Wu, and  
524 Jun Liu. Chartsketcher: Reasoning with multimodal feedback and reflection for chart understand-  
525 ing. *arXiv preprint arXiv:2505.19076*, 2025.

526 Mohammed Saidul Islam, Raian Rahman, Ahmed Masry, Md Tahmid Rahman Laskar, Mir Tafseer  
527 Nayeem, and Enamul Hoque. Are large vision language models up to the challenge of chart  
528 comprehension and reasoning? an extensive investigation into the capabilities and limitations of  
529 l4lms. *arXiv preprint arXiv:2406.00257*, 2024.

530 Albert Q Jiang, Alexandre Sablayrolles, Antoine Roux, Arthur Mensch, Blanche Savary, Chris  
531 Bamford, Devendra Singh Chaplot, Diego de las Casas, Emma Bou Hanna, Florian Bressand, et al.  
532 Mixtral of experts. *arXiv preprint arXiv:2401.04088*, 2024.

533 Daniel Kahneman. *Thinking, fast and slow*. macmillan, 2011.

540 Kenton Lee, Mandar Joshi, Iulia Raluca Turc, Hexiang Hu, Fangyu Liu, Julian Martin Eisenschlos,  
 541 Urvashi Khandelwal, Peter Shaw, Ming-Wei Chang, and Kristina Toutanova. Pix2struct: Screenshot  
 542 parsing as pretraining for visual language understanding. In *International Conference on Machine  
 543 Learning*, pp. 18893–18912. PMLR, 2023.

544 Hunter Lightman, Vineet Kosaraju, Yuri Burda, Harrison Edwards, Bowen Baker, Teddy Lee, Jan  
 545 Leike, John Schulman, Ilya Sutskever, and Karl Cobbe. Let’s verify step by step. In *The Twelfth  
 546 International Conference on Learning Representations*, 2023.

547 Haotian Liu, Chunyuan Li, Qingyang Wu, and Yong Jae Lee. Visual instruction tuning. *Advances in  
 548 neural information processing systems*, 36:34892–34916, 2023.

549 Yan Ma, Linge Du, Xuyang Shen, Shaoxiang Chen, Pengfei Li, Qibing Ren, Lizhuang Ma, Yuchao  
 550 Dai, Pengfei Liu, and Junjie Yan. One rl to see them all: Visual triple unified reinforcement  
 551 learning. *arXiv preprint arXiv:2505.18129*, 2025.

552 Ahmed Masry, Do Xuan Long, Jia Qing Tan, Shafiq Joty, and Enamul Hoque. Chartqa: A bench-  
 553 mark for question answering about charts with visual and logical reasoning. *arXiv preprint  
 554 arXiv:2203.10244*, 2022.

555 Ahmed Masry, Parsa Kavehzadeh, Xuan Long Do, Enamul Hoque, and Shafiq Joty. Unichart: A  
 556 universal vision-language pretrained model for chart comprehension and reasoning. *arXiv preprint  
 557 arXiv:2305.14761*, 2023.

558 Ahmed Masry, Megh Thakkar, Aayush Bajaj, Aaryaman Kartha, Enamul Hoque, and Shafiq  
 559 Joty. Chartgemma: Visual instruction-tuning for chart reasoning in the wild. *arXiv preprint  
 560 arXiv:2407.04172*, 2024.

561 Fanqing Meng, Wenqi Shao, Quanfeng Lu, Peng Gao, Kaipeng Zhang, Yu Qiao, and Ping Luo.  
 562 Chartassisstant: A universal chart multimodal language model via chart-to-table pre-training and  
 563 multitask instruction tuning. *arXiv preprint arXiv:2401.02384*, 2024.

564 Fanqing Meng, Lingxiao Du, Zongkai Liu, Zhixiang Zhou, Quanfeng Lu, Daocheng Fu, Tiancheng  
 565 Han, Botian Shi, Wenhui Wang, Junjun He, et al. Mm-eureka: Exploring the frontiers of multimodal  
 566 reasoning with rule-based reinforcement learning. *arXiv preprint arXiv:2503.07365*, 2025.

567 Minheng Ni, Zhengyuan Yang, Linjie Li, Chung-Ching Lin, Kevin Lin, Wangmeng Zuo, and Lijuan  
 568 Wang. Point-rft: Improving multimodal reasoning with visually grounded reinforcement finetuning.  
 569 *arXiv preprint arXiv:2505.19702*, 2025.

570 OpenAI. Gpt-5 system card. Technical report, OpenAI, 2025. URL <https://openai.com/index/gpt-5-system-card/>. PDF available; Accessed: 2025-08-11.

571 Aaron Parisi, Yao Zhao, and Noah Fiedel. Talm: Tool augmented language models. *arXiv preprint  
 572 arXiv:2205.12255*, 2022.

573 Shishir G Patil, Tianjun Zhang, Xin Wang, and Joseph E Gonzalez. Gorilla: Large language  
 574 model connected with massive apis. *Advances in Neural Information Processing Systems*, 37:  
 575 126544–126565, 2024.

576 Alec Radford, Jong Wook Kim, Chris Hallacy, Aditya Ramesh, Gabriel Goh, Sandhini Agarwal,  
 577 Girish Sastry, Amanda Askell, Pamela Mishkin, Jack Clark, et al. Learning transferable visual  
 578 models from natural language supervision. In *International conference on machine learning*, pp.  
 579 8748–8763. PmLR, 2021.

580 Sara Sabour, Nicholas Frosst, and Geoffrey E Hinton. Dynamic routing between capsules. *Advances  
 581 in neural information processing systems*, 30, 2017.

582 Timo Schick, Jane Dwivedi-Yu, Roberto Dessì, Roberta Raileanu, Maria Lomeli, Eric Hambro, Luke  
 583 Zettlemoyer, Nicola Cancedda, and Thomas Scialom. Toolformer: Language models can teach  
 584 themselves to use tools. *Advances in Neural Information Processing Systems*, 36:68539–68551,  
 585 2023.

594 Zhihong Shao, Peiyi Wang, Qihao Zhu, Runxin Xu, Junxiao Song, Xiao Bi, Haowei Zhang,  
 595 Mingchuan Zhang, YK Li, Yang Wu, et al. Deepseekmath: Pushing the limits of mathemat-  
 596 ical reasoning in open language models. *arXiv preprint arXiv:2402.03300*, 2024.

597

598 Noah Shinn, Federico Cassano, Ashwin Gopinath, Karthik Narasimhan, and Shunyu Yao. Reflexion:  
 599 Language agents with verbal reinforcement learning. *Advances in Neural Information Processing  
 600 Systems*, 36:8634–8652, 2023.

601 Zhaochen Su, Linjie Li, Mingyang Song, Yunzhuo Hao, Zhengyuan Yang, Jun Zhang, Guanjie Chen,  
 602 Jiawei Gu, Juntao Li, Xiaoye Qu, et al. Openthinking: Learning to think with images via visual  
 603 tool reinforcement learning. *arXiv preprint arXiv:2505.08617*, 2025.

604

605 Sanjay Subramanian, Medhini Narasimhan, Kushal Khangaonkar, Kevin Yang, Arsha Nagrani,  
 606 Cordelia Schmid, Andy Zeng, Trevor Darrell, and Dan Klein. Modular visual question answering  
 607 via code generation. *arXiv preprint arXiv:2306.05392*, 2023.

608 Dídac Surís, Sachit Menon, and Carl Vondrick. Viperpt: Visual inference via python execution  
 609 for reasoning. In *Proceedings of the IEEE/CVF international conference on computer vision*, pp.  
 610 11888–11898, 2023.

611

612 Hugo Touvron, Thibaut Lavril, Gautier Izacard, Xavier Martinet, Marie-Anne Lachaux, Timothée  
 613 Lacroix, Baptiste Rozière, Naman Goyal, Eric Hambro, Faisal Azhar, et al. Llama: Open and  
 614 efficient foundation language models. *arXiv preprint arXiv:2302.13971*, 2023.

615 Xuezhi Wang, Jason Wei, Dale Schuurmans, Quoc Le, Ed Chi, Sharan Narang, Aakanksha Chowdh-  
 616 ery, and Denny Zhou. Self-consistency improves chain of thought reasoning in language models.  
 617 *arXiv preprint arXiv:2203.11171*, 2022.

618

619 Zirui Wang, Mengzhou Xia, Luxi He, Howard Chen, Yitao Liu, Richard Zhu, Kaiqu Liang, Xindi  
 620 Wu, Haotian Liu, Sadhika Malladi, et al. Charxiv: Charting gaps in realistic chart understanding in  
 621 multimodal llms. *Advances in Neural Information Processing Systems*, 37:113569–113697, 2024.

622

623 Jason Wei, Xuezhi Wang, Dale Schuurmans, Maarten Bosma, Fei Xia, Ed Chi, Quoc V Le, Denny  
 624 Zhou, et al. Chain-of-thought prompting elicits reasoning in large language models. *Advances in  
 625 neural information processing systems*, 35:24824–24837, 2022.

626

627 Renqiu Xia, Bo Zhang, Hancheng Ye, Xiangchao Yan, Qi Liu, Hongbin Zhou, Zijun Chen, Peng Ye,  
 628 Min Dou, Botian Shi, et al. Chartx & chartvilm: A versatile benchmark and foundation model for  
 629 complicated chart reasoning. *arXiv preprint arXiv:2402.12185*, 2024.

630

631 Zhengzhuo Xu, Sinan Du, Yiyan Qi, Chengjin Xu, Chun Yuan, and Jian Guo. Chartbench: A  
 632 benchmark for complex visual reasoning in charts. *arXiv preprint arXiv:2312.15915*, 2023.

633

634 Zhengzhuo Xu, Bowen Qu, Yiyan Qi, Sinan Du, Chengjin Xu, Chun Yuan, and Jian Guo. Chart-  
 635 moe: Mixture of diversely aligned expert connector for chart understanding. *arXiv preprint  
 636 arXiv:2409.03277*, 2024.

637

638 Cheng Yang, Chufan Shi, Yixin Liu, Bo Shui, Junjie Wang, Mohan Jing, Linran Xu, Xinyu Zhu,  
 639 Siheng Li, Yuxiang Zhang, et al. Chartmimic: Evaluating lmm’s cross-modal reasoning capability  
 640 via chart-to-code generation. *arXiv preprint arXiv:2406.09961*, 2024.

641

642 Shunyu Yao, Dian Yu, Jeffrey Zhao, Izhak Shafran, Tom Griffiths, Yuan Cao, and Karthik Narasimhan.  
 643 Tree of thoughts: Deliberate problem solving with large language models. *Advances in neural  
 644 information processing systems*, 36:11809–11822, 2023a.

645

646 Shunyu Yao, Jeffrey Zhao, Dian Yu, Nan Du, Izhak Shafran, Karthik Narasimhan, and Yuan Cao.  
 647 React: Synergizing reasoning and acting in language models. In *International Conference on  
 648 Learning Representations (ICLR)*, 2023b.

649

650 Yi-Fan Zhang, Xingyu Lu, Shukang Yin, Chaoyou Fu, Wei Chen, Xiao Hu, Bin Wen, Kaiyu Jiang,  
 651 Changyi Liu, Tianke Zhang, Haonan Fan, Kaibing Chen, Jiankang Chen, Haojie Ding, Kaiyu Tang,  
 652 Zhang Zhang, Liang Wang, Fan Yang, Tingting Gao, and Guorui Zhou. Thyme: Think beyond  
 653 images, 2025. URL <https://arxiv.org/abs/2508.11630>.

648 Shitian Zhao, Haoquan Zhang, Shaoheng Lin, Ming Li, Qilong Wu, Kaipeng Zhang, and Chen Wei.  
 649 Pyvision: Agentic vision with dynamic tooling. *arXiv preprint arXiv:2507.07998*, 2025a.  
 650  
 651 Xuanle Zhao, Xianzhen Luo, Qi Shi, Chi Chen, Shuo Wang, Zhiyuan Liu, and Maosong Sun.  
 652 Chartcoder: Advancing multimodal large language model for chart-to-code generation. *arXiv  
 653 preprint arXiv:2501.06598*, 2025b.  
 654  
 655 Yaowei Zheng, Junting Lu, Shenzhi Wang, Zhangchi Feng, Dongdong Kuang, and Yuwen Xiong.  
 656 Easyr1: An efficient, scalable, multi-modality rl training framework. [https://github.com/  
 657 hiyouga/EasyR1](https://github.com/hiyouga/EasyR1), 2025. GitHub repository.

## 658 THE USE OF LARGE LANGUAGE MODELS

660 We used Gemini 2.5 Pro for the following limited purposes: (i) language polishing of paragraphs;  
 661 (ii) generating boilerplate code for plotting; and (iii) drafting figure captions. All scientific claims,  
 662 methods, and results were conceived, verified, and validated by the authors. We manually checked  
 663 and reproduced any outputs suggested by the LLM. No confidential or identifying information was  
 664 provided to the LLM service.

## 666 A DETAILED ANALYSIS OF FIXED-STRATEGY EXPERIMENTS

668 **Experimental Setting.** To create our specialist model, we fine-tuned Qwen2.5-VL-7B using a  
 669 Supervised Fine-Tuning (SFT) approach on the ChartX validation set Xia et al. (2024). This dataset  
 670 consists of approximately 4,800 highly structured charts well-suited for programmatic analysis. We  
 671 then evaluated this specialized model’s generalization ability across four diverse test suites, each  
 672 containing 500 samples designed to span a spectrum of difficulty and style:

- 674 • **In-Domain (ChartX Xia et al. (2024)):** A stratified sample from the official test set,  
 675 ensuring equal representation of chart types (e.g., bar, line, pie). This measures performance  
 676 on data from the same distribution as the training set.
- 677 • **Near-Domain (ChartBench Xu et al. (2023)):** A similarly stratified sample from Chart-  
 678 Bench. This benchmark, while out-of-domain (OOD), shares structural and stylistic similar-  
 679 ities with ChartX, testing for near-transfer capabilities.
- 680 • **Far-Domain (ChartQA Masry et al. (2022)):** A random sample from the human-annotated  
 681 portion of the test set. These examples often require deeper, qualitative reasoning, posing a  
 682 rigorous challenge to purely quantitative methods.
- 683 • **Far-Domain (CharXiv Wang et al. (2024)):** A random sample from CharXiv, which  
 684 contains "in-the-wild" scientific charts with significant visual complexity and stylistic  
 685 diversity. This serves as a stress test for generalization.

686 This multi-faceted evaluation was designed to reveal how a strategy optimized for clean, struc-  
 687 tured data would perform when confronted with the ambiguities and complexities of real-world  
 688 visualizations.

690 **Detailed Analysis.** The results in Table 8 reveal a sharp dichotomy in generalization performance.  
 691 The code-based specialist (SFT, Code-based CoT) excelled on structured data, achieving an  
 692 impressive **71.6%** on ChartX. However, this rigid strategy proved brittle when generalized, with  
 693 accuracy plummeting on complex charts like CharXiv to just **18.4%**. This shows how reasoning  
 694 patterns effective for simple charts become detrimental when misapplied. Furthermore, this failure  
 695 is not a simple matter of competence that can be fixed with more training. Optimizing the policy  
 696 with reinforcement learning (RL) or maximizing coding skill on a vast dataset (CPT + RL) failed to  
 697 resolve this core conflict.

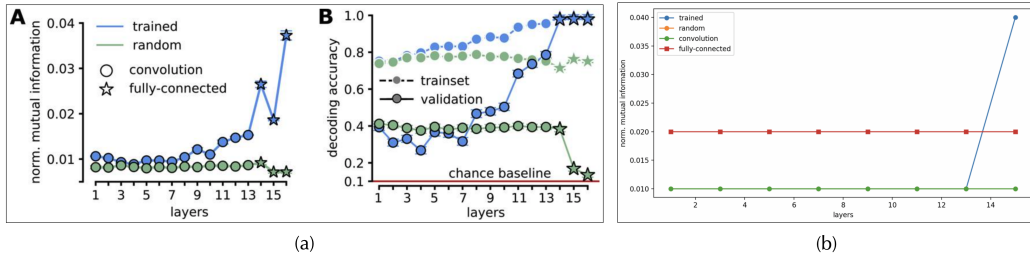
## 698 B CASE STUDY: FAILURE DUE TO NUMERICAL HALLUCINATION

700 As discussed in Section 3, a critical failure mode for rigid, code-based strategies is *numerical  
 701 hallucination*. This occurs when the model incorrectly perceives the visual information in a chart

**Table 8:** Detailed performance of "One-Size-Fits-All" Strategies. This table provides the full numerical data visualized in Figure 2 in the main text. All models are fine-tuned (SFT or RL) on the ChartX validation set. The CPT model first undergoes continued pre-training on Chart2Code-160k Zhao et al. (2025b) to enhance its core chart-to-code ability. Despite optimization, no single strategy excels across all benchmarks, revealing a fundamental performance trade-off.

Prompt Strategy	Training Method	ChartX	ChartBench	ChartQA	CharXiv	Average
Standard CoT	Base Model	59.8	51.6	80.4	38.2	58.7
	SFT on ChartX	69.8	56.2	72.0	37.2	58.8
	RL on ChartX	63.0	53.0	<b>81.6</b>	<b>39.4</b>	59.3
Code-as-Thought	Base Model	62.6	53.4	74.8	29.8	55.2
	SFT on ChartX	<b>71.6</b>	<b>56.8</b>	68.2	18.4	53.8
	RL on ChartX	66.6	55.8	78.0	37.0	<b>59.4</b>
	CPT + RL on ChartX	69.2	54.0	68.6	32.0	56.0

and generates flawed code based on this misperception. The model then proceeds to execute its own flawed logic, leading to an answer that is logically consistent with its internal (wrong) representation but factually incorrect.



[Question]: How many number of datapoints for convolution in the figure A?

[Ground Truth]: 26

[Answer]: The code is ````python\n[code]\n````. The total number of datapoints for convolution in the figure A is 8. \boxed{8}

**Figure 7: Failure of a Rigid Code-Based Strategy on a CharXiv Example.** The model is tasked with analyzing the original chart (a) from the CharXiv dataset. It generates Python code (indicated in the red box) to extract the data, but this code hallucinates an incorrect data structure. Chart (b) is the visualization produced by *executing the model’s flawed code*. The model then faithfully reasons over its own erroneous chart (b) to arrive at the answer ‘8’, a stark deviation from the ground truth of 26. This case exemplifies how a rigid code-based approach can fail by building logical conclusions on a foundation of numerical hallucination.

## C ANNOTATION FRAMEWORK FOR VISUAL PROGRAMMABILITY

To train a model capable of recognizing Visual Programmability, we developed a rigorous annotation framework grounded in expert human judgment. We chose this approach because the boundary between visual and symbolic representation is fundamentally cognitive; it involves nuanced, tacit knowledge that is difficult to capture with purely algorithmic rules.

### C.1 GUIDING PRINCIPLE

We built our methodology around a single, functional question for annotators: *“Does a code-based representation preserve the essential information required to correctly answer this question?”* This principle ensures that every label is context-aware, reflecting how the task depends on both the chart’s properties and the user’s specific query.

### C.2 ASSESSMENT CRITERIA

Annotators evaluated each chart-question pair using a two-step assessment designed to mirror the decision-making process we want our model to learn.

756

- 757 • **Primary Assessment: Information Preservation.** The core question was whether the  
758 chart’s essential information could be faithfully translated into code. Annotators considered  
759 if the underlying data could be reliably extracted from visual elements (e.g., bar heights, point  
760 positions) and if this programmatic format would retain everything needed to answer the  
761 question. If critical information was lost in this translation—such as the meaning conveyed  
762 by complex annotations, visual metaphors, or specific color gradients—the instance was  
763 marked as having low programmability for that task.
- 764 • **Secondary Assessment: Reconstruction Feasibility.** As a practical test, annotators per-  
765 formed a “mental compilation.” They envisioned how the chart might be programmatically  
766 recreated using a standard plotting library like Matplotlib. If key visual elements or context  
767 could not be captured in this hypothetical reconstruction, it served as a strong signal for low  
768 programmability.

769 **C.3 ANNOTATION PROCESS AND QUALITY CONTROL**

770 To ensure the quality and consistency of our dataset, we followed a structured process.

771

- 772 • **Binary Categorization.** For practical model training, we classified each instance into  
773 one of two categories: **high programmability** (suitable for code-based reasoning) or **low  
774 programmability** (requires direct visual reasoning). This binary choice frames the model’s  
775 learning objective as a clear, decisive action.
- 776 • **Systematic Guidelines.** All annotations were guided by a detailed rulebook. In ambiguous  
777 or boundary cases, annotators were instructed to be conservative, prioritizing the integrity of  
778 the visual information over forcing a programmatic representation.
- 779 • **Quality Assurance.** We regularly reviewed batches of annotated samples to ensure ad-  
780 herence to our guidelines. This iterative validation process helped maintain high levels of  
781 consistency and quality throughout the dataset.

782 By grounding our dataset in this human-centric process, we provide our model with a supervisory  
783 signal that reflects the nuances of human cognition. This enables it to learn a flexible, adaptive policy  
784 for chart understanding that moves beyond the limitations of rigid, rule-based systems.

785 **D EXPERIMENTAL SETUP DETAILS**

786

787 **Training Data.** Our training is based on the ChartMimic Yang et al. (2024) dataset, which contains  
788 4,800 diverse chart–code pairs without QA. To support adaptive learning, we expand this dataset  
789 by generating new question–answer pairs with Gemini-2.5-Flash Comanici et al. (2025), using  
790 the prompts in Appendix F. This yields a balanced training set that includes charts well-suited for  
791 code-based reasoning as well as those demanding direct visual interpretation.

792

793 **Evaluation Benchmarks.** We evaluate across four benchmarks chosen to span a wide range of  
794 Visual Programmability:

795

- 796 • **ChartX** Xia et al. (2024): high-programmability charts (1,152 structured plots), ideal for  
797 testing code-based reasoning.
- 798 • **ChartBench (NQA)** Xu et al. (2023): numerical reasoning where data points are not  
799 explicitly labeled; we use 2,000 NQA samples to test programmatic extraction from visual  
800 cues.
- 801 • **ChartQA** Masry et al. (2022): 2,396 real-world charts with human/template questions,  
802 covering basic retrieval to multi-step reasoning.
- 803 • **CharXiv** Wang et al. (2024): low-programmability, in-the-wild scientific charts (1,323  
804 plots) stressing robustness when code is unreliable.

805

806 **Training Details.** We initialize Qwen2.5-VL-7B and train it with EasyR1 Zheng et al. (2025) using  
807 GRPO (objective in Appendix G), guided by the multi-component reward in Eq. 2. After validation  
808 tuning, weights are set to: answer accuracy  $w_{\text{acc}}=0.8$ , decision appropriateness  $w_{\text{decision}}=0.3$ , data

810 fidelity  $w_{\text{data}}=0.15$ , and format compliance  $w_{\text{format}}=0.05$ . All prompts appear in Appendix F. A  
 811 complete list of hyperparameters and implementation specifics is provided in Appendix J.  
 812

813

814

## E DATA ACCURACY REWARD IMPLEMENTATION

815

816

817 The Data Accuracy Reward ( $r_{\text{data}}$ ) is a critical component for ensuring that the model’s generated  
 818 code is not only syntactically correct but also faithfully extracts the data from the chart. This reward  
 819 is calculated by comparing the DataFrame generated by the model’s code against a ground-truth CSV.  
 820 The full process is detailed in Algorithm 1.

821

822

---

**Algorithm 1** Data Accuracy Reward Computation
 

---

823  
**Require:** Generated code  $c_{\text{pred}}$ , Ground truth CSV  $\text{csv}_{\text{gt}}$   
**Ensure:** Data accuracy reward  $r_{\text{data}}$

824 1: Extract DataFrame construction code from  $c_{\text{pred}}$  using AST parsing  
 825 2:  $\text{DF}_{\text{pred}} \leftarrow \text{CONSTRUCTDATAFRAME}(\text{extracted\_data})$   
 826 3:  $\text{DF}_{\text{gt}} \leftarrow \text{PARSECSV}(\text{csv}_{\text{gt}})$   
 827 4: **if**  $\text{DF}_{\text{pred}}$  is None or  $\text{DF}_{\text{gt}}$  is None **then**  
 828     **return** 0.0  
 829 5:     **end if**  
 830 6:     **end if**  
 831 7:     **return**  $r_{\text{data}}$  ▷ Column Completeness Score  
 832 8:      $\text{matched\_cols} \leftarrow 0$   
 833 9:     **for** each column  $c_{\text{ref}}$  in  $\text{DF}_{\text{gt}}$  **do**  
 834          $c_{\text{ref}}^{\text{norm}} \leftarrow \text{NORMALIZE}(c_{\text{ref}})$  ▷ Remove spaces, lowercase  
 835          $\text{best\_match} \leftarrow \text{FUZZYMATCH}(c_{\text{ref}}^{\text{norm}}, \text{DF}_{\text{pred}}.\text{columns})$   
 836         **if**  $\text{match\_score} > 50$  **then**  
 837              $\text{matched\_cols} \leftarrow \text{matched\_cols} + 1$   
 838         **end if**  
 839     **end for**  
 840 16:      $r_{\text{col}} \leftarrow \text{matched\_cols} / \text{len}(\text{DF}_{\text{gt}}.\text{columns})$  ▷ Row Completeness Score  
 841 18:      $r_{\text{row}} \leftarrow \mathbb{1}[\text{len}(\text{DF}_{\text{pred}}) = \text{len}(\text{DF}_{\text{gt}})]$  ▷ Value Accuracy Score  
 842 19:      $\text{total\_accuracy} \leftarrow 0$   
 843 20:      $\text{compared\_cols} \leftarrow 0$   
 844 22:     **for** each matched column pair  $(c_{\text{pred}}, c_{\text{gt}})$  **do**  
 845          $\text{correct\_values} \leftarrow 0$   
 846         **for** each row  $i$  in  $\min(\text{len}(\text{DF}_{\text{pred}}), \text{len}(\text{DF}_{\text{gt}}))$  **do**  
 847             **if**  $\text{COMPAREVALUES}(\text{DF}_{\text{pred}}[c_{\text{pred}}][i], \text{DF}_{\text{gt}}[c_{\text{gt}}][i])$  **then**  
 848                  $\text{correct\_values} \leftarrow \text{correct\_values} + 1$   
 849             **end if**  
 850         **end for**  
 851          $\text{col\_accuracy} \leftarrow \text{correct\_values} / \text{num\_comparisons}$   
 852          $\text{total\_accuracy} \leftarrow \text{total\_accuracy} + \text{col\_accuracy}$   
 853          $\text{compared\_cols} \leftarrow \text{compared\_cols} + 1$   
 854     **end for**  
 855 33:      $r_{\text{values}} \leftarrow \text{total\_accuracy} / \text{compared\_cols}$  ▷ Combined Data Accuracy Score  
 856 34:      $r_{\text{data}} \leftarrow 0.2 \cdot r_{\text{col}} + 0.1 \cdot r_{\text{row}} + 0.7 \cdot r_{\text{values}}$   
 857 36:     **return**  $r_{\text{data}}$   
 858

---

859

860

861

862

863

The  $\text{COMPAREVALUES}$  function is designed to be robust. For numerical values, it uses a relative tolerance of  $10^{-2}$  to handle minor extraction or floating-point discrepancies. For textual values, it performs case-insensitive, normalized string matching. It also correctly handles NaN values, returning true only if both values are NaN.

864 **F DETAILED PROMPT SPECIFICATIONS**  
865866 This section details the key prompts used for data generation and model training. The prompt  
867 for generating synthetic question-answer pairs is presented in Prompt F. The baseline prompts for  
868 direct Chain-of-Thought and mandatory code-based reasoning are shown in Prompt F and Prompt F,  
869 respectively. Finally, the master prompt that guides our adaptive model to learn strategy selection is  
870 detailed in Prompt F.  
871872 **Prompt for Synthetic Question-Answer Pair Generation**  
873

```

874 You are a specialized generator of chart comprehension
875 questions. Using (i) a chart graphic and (ii) the Python
876 code that creates it, formulate **one** question with
877 its correct answer.
878 ### Guidelines
879 1. Answers must come from chart observation and code
880 understanding
881 2. Provide exactly one brief, precise response with
882 **no additional details**
883 3. Avoid multiple choice, yes/no, or lengthy
884 descriptive formats
885 4. Emphasize questions requiring data interpretation expertise
886 5. Keep answers short (numbers, percentages, names, dates,
887 or brief terms)
888 ### Question Categories
889 #### **Numerical Operations**
890 - **Counting Tasks**: Enumerate items, groups, or elements
891 with properties
892 - **Basic Mathematics**: Addition, subtraction, multiplication,
893 division
894 - **Descriptive Statistics**: Average, median, mode, range,
895 maximum, minimum
896 - **Ratio Analysis**: Proportional relationships
897 between categories
898 - **Conditional Analysis**: Elements meeting specific
899 requirements
900 - **Multi-step Problems**: Combined computational
901 operations
902 #### **Object Recognition**
903 - **Ranking Identification**: Highest or lowest performing
904 entities
905 - **Peak Value Location**: Items with extreme measurements
906 - **Group Classification**: Category membership identification
907 - **Time-based Analysis**: Performance identification across
908 periods
909 - **Benchmark Comparison**: Items relative to specific
910 standards
911 #### **Comparison Tasks**
912 - **Head-to-head Analysis**: Direct comparison between entities
913 - **Position Ranking**: Order determination in sequences
914 - **Variation Analysis**: Largest differences between items
915 #### **Temporal Analysis**
916 - **Trend Identification**: Increase/decrease periods
917 - **Change Detection**: Significant transition moments
918 - **Pattern Analysis**: Cyclical or seasonal behaviors
919 ### Answer Types
920 - **Numeric**: '92', '4.2', '17%'
921 - **Monetary**: '$2,100', '£1,400'

```

```

918
919     - **Names**: 'Samsung', 'India', '2022'
920     - **Categories**: 'Transportation', 'Media'
921     - **Time**: 'August', 'Q4', '2018'
922     - **Ratios**: '3:5', '1.7'
923     ### Output Format
924     ````json
925     {"question": "Question text here", "answer": "Short answer"}
926     ````

927     ### Task
928     **Chart Image**: <image>
929     **Python Code**: {python_files}
930     Develop one JSON question-answer pair.

```

### Baseline Chain-of-Thought (CoT) Prompt

Carefully examine this chart. Based on your observations, answer the question. Let's reason step by step, then put your final answer under format \boxed{ }.

### Code-based Chain-of-Thought (Code-CoT) Prompt

You must carefully examine the chart and the question. First redraw the image using Python code. This code should aim to focus on data accuracy and basic chart type representation. The code must be runnable. Before any plotting, import pandas and construct one 'pandas.DataFrame' named 'chart\_data' that contains all raw numerical data you will use. The DataFrame must include appropriate column names and keep the original row order. Then describe your step-by-step thought process and answer the question using a single word or phrase and put it under format \boxed{ }.

### Master Prompt for the Adaptive Reasoning Framework

You are an expert at analyzing charts and answering questions about them. You have two powerful approaches, with code-based analysis being your preferred method when applicable.

#### ## Core Principle

Code-based analysis is highly effective and should be your first choice when charts contain extractable data. Code provides precision, reproducibility, and often superior accuracy compared to visual estimation.

#### ## Approach Selection Examples

\*\*Example 1:\*\* Bar chart with clear axis labels and readable values

- Question: "What's the average value across all bars?"
- Best Choice: <CODE> (Perfect for extracting values and calculating precisely)

\*\*Example 2:\*\* Complex 3D visualization or heavily artistic infographic

- Question: "What trend does this show?"
- Best Choice: <DIRECT> (Data extraction would be unreliable here)

```

972
973     ## When to Use Each Approach
974     ### Use <CODE> When Charts Are Analyzable:
975     - **Any Standard Chart**: Bar, line, pie, scatter,
976     histogram - even if slightly messy
977     - **Readable Data Points**: If you can see numbers
978     or estimate from gridlines - **use code!**
979     - **Clear Structure**: Regular patterns, axes,
980     legends - perfect for code extraction
981     - **Questions Needing Precision**: Calculations, comparisons,
982     trends - code gives exact answers
983     - **Moderate Complexity**: Don't avoid code just because
984     extraction takes effort - be brave!
985
986     ### Use <DIRECT> Only When Code Is Truly Impractical:
987     - **Extremely Artistic/Stylized**: Heavy design elements
988     completely obscure data structure
989     - **No Readable Scale**: Completely missing or unintelligible
990     axes
991     - **Pure Qualitative**: Questions only about general patterns,
992     not specific values
993     - **Severely Distorted**: 3D effects or perspectives that make
994     extraction impossible
995
996     ## **Decision Framework**
997     **Step 1: Code Preference Check**
998     - Can I see any numerical data or gridlines? → **TRY <CODE>**
999     - Are there clear bars, lines, or data points? → **TRY <CODE>**
1000    - Would precise calculations help answer this question? →
1001    **TRY <CODE>**
1002
1003    **Step 2: Only if Step 1 fails**
1004    - Is the chart purely artistic with no extractable structure?
1005    → Use <DIRECT>
1006    - Is the question purely qualitative? → Use <DIRECT>
1007
1008    ## Response Format
1009    **First, make your choice with confidence:**
1010    - For code-assisted analysis: output <CODE>
1011    - For direct analysis: output <DIRECT>
1012
1013    ### If Using Code-Assisted Analysis (<CODE>):
1014    **Start with**: <CODE>
1015    Then proceed with your analysis using code as helpful. Before
1016    any coding, import pandas and construct one 'pandas.DataFrame',
1017    named 'chart_data' that contains all raw numerical data you
1018    will use. The DataFrame must include appropriate column names
1019    and keep the original row order. You may:
1020    - Redraw/recreate the chart data for comprehensive analysis
1021    - Use code for calculations, comparisons, or data processing
1022    - Combine visual observations with computational analysis
1023    - Focus on the most relevant chart elements for the question
1024
1025    *Note: Choose the code approach that best fits the chart and
1026    question - full redrawing, partial extraction, or targeted
1027    calculations.*
```

```

1026
1027    **Start with**: <DIRECT>
1028    Then provide your reasoning and analysis in the most effective
1029    way for the question. Consider:
1030    - Key observations and findings from the chart
1031    - Your reasoning process and logical steps
1032    - Relevant patterns or trends you identify
1033
1034    ## Final Answer Format
1035    Every response MUST end with \\boxed{your_answer}
1036
1037    Now analyze the given chart and question. Choose your approach
1038    based on the chart's extractability and the question's
1039    requirements.

```

## G GRPO OBJECTIVE AND UPDATE DETAILS

We employ Group Relative Policy Optimization (GRPO) Shao et al. (2024), a policy-gradient method that leverages group-normalized advantages and PPO-style clipping. For each training instance  $x$ , we sample a group of  $G$  responses  $\{r_i\}_{i=1}^G$  from the previous policy  $\pi_{\text{old}}$ , evaluate them with our reward  $R$ , and update the current policy  $\pi_\theta$  by maximizing:

$$J_{\text{GRPO}}(\theta) = \mathbb{E} \left[ \sum_{i=1}^G \min \left( \frac{\pi_\theta(r_i|x)}{\pi_{\text{old}}(r_i|x)} A_i, \text{clip} \left( \frac{\pi_\theta(r_i|x)}{\pi_{\text{old}}(r_i|x)}, 1-\epsilon, 1+\epsilon \right) A_i \right) - \beta D_{\text{KL}}(\pi_\theta \| \pi_{\text{ref}}) \right], \quad (3)$$

where the group-normalized advantage is

$$A_i = \frac{R(r_i, \phi_i) - \text{mean}(\{R(\xi, \phi)\}_{\xi=1}^G)}{\text{std}(\{R(\xi, \phi)\}_{\xi=1}^G)}. \quad (4)$$

Here,  $\epsilon$  controls the clipping range, and  $\beta$  weights the KL penalty against a reference policy  $\pi_{\text{ref}}$ . In our final configuration, we set  $\beta=0$  (KL-free), focusing purely on the group-relative signal.

### Practical Notes.

- **Sampling.** For each  $x$ , draw  $G$  responses from  $\pi_{\text{old}}$ ; compute rewards and  $A_i$  using the group statistics.
- **Clipped update.** Define ratio  $\rho_i = \pi_\theta(r_i|x)/\pi_{\text{old}}(r_i|x)$  and apply  $\min(\rho_i A_i, \text{clip}(\rho_i, 1-\epsilon, 1+\epsilon) A_i)$ .
- **No-KL setup.** Use  $\beta=0$ ; we found this configuration works well with verifiable rewards.

## H BROADER IMPLICATIONS AND FUTURE DIRECTIONS

Our work on adaptive chart reasoning, while focused on a specific domain, offers insights into a broader challenge in artificial intelligence: developing systems that can flexibly navigate between different problem-solving strategies. Just as humans alternate between rapid, intuitive pattern recognition and slower, deliberate symbolic reasoning Kahneman (2011), future AI systems must master not only individual skills but also the meta-level ability to select the right tool for the job.

**From Modality Fusion to Method Fusion.** Much of the research in multimodal AI has centered on *modality fusion*—the effective combination of information from different sensory channels. Our framework points towards a complementary and perhaps equally important paradigm: *method fusion*. This refers to the ability to select and combine different reasoning strategies (e.g., visual-perceptual vs. symbolic-programmatic) even when operating within a single modality. The challenge is not only to perceive the world through multiple senses but to think about it through multiple "lenses," fluidly shifting between holistic, pattern-based analysis and precise, step-by-step decomposition as the problem demands.

1080     **Competence Awareness as a Foundational Capability.** A key takeaway from our research is that  
 1081     models can be trained to recognize the boundaries of their own competence with respect to specific  
 1082     methods. This nascent form of meta-cognitive awareness—knowing not just *how* to solve a problem,  
 1083     but knowing *which* of its available methods is most likely to succeed—is a fundamental prerequisite  
 1084     for robust and reliable AI. We foresee that future general-purpose systems will need to develop richer  
 1085     internal models of their own capabilities, enabling them to make more dependable strategy selections  
 1086     when faced with novel tasks.

1087     **Limitations and Key Future Directions.** While our adaptive framework represents a significant  
 1088     step, its current limitations highlight critical areas for future research that build directly upon our  
 1089     findings.

- 1091     • **Granular and Hybrid Reasoning:** The current decision-making process is a binary choice  
 1092     between "code" and "direct" reasoning. This could be extended to a more granular **hybrid**  
 1093     **model**, where code is used for reliable data extraction while visual reasoning concurrently  
 1094     interprets qualitative patterns from the same chart. Furthermore, assessing programmability  
 1095     at the chart-level is coarse; future models could learn to perform **region-based assessment**,  
 1096     applying different strategies to different parts of a single complex figure.
- 1097     • **Expanding the Vocabulary of Formal Reasoning:** Our model's "Code as Thought" process  
 1098     is currently centered on data analysis logic. A natural evolution is to expand the scope of this  
 1099     *native* formal reasoning. Instead of orchestrating external tools, future work could enrich  
 1100     the model's internal symbolic language to encompass other formalisms, such as the logic of  
 1101     signal processing for time-series charts or graph-theoretic principles for network diagrams.  
 1102     This would extend the reach of the model's innate symbolic capabilities, allowing it to  
 1103     tackle a wider range of problems programmatically without breaking the "native reasoning"  
 1104     paradigm.
- 1105     • **Self-Supervised Policy Learning:** A key challenge is reducing the reliance on annotated  
 1106     training data for programmability. A promising direction is developing **self-supervised**  
 1107     **methods** where the model learns the decision boundary by correlating its choice of strategy  
 1108     with final task success. This would effectively teach the model to recognize the reliable  
 1109     application range of its own internal methods without requiring explicit human-provided  
 1110     labels.

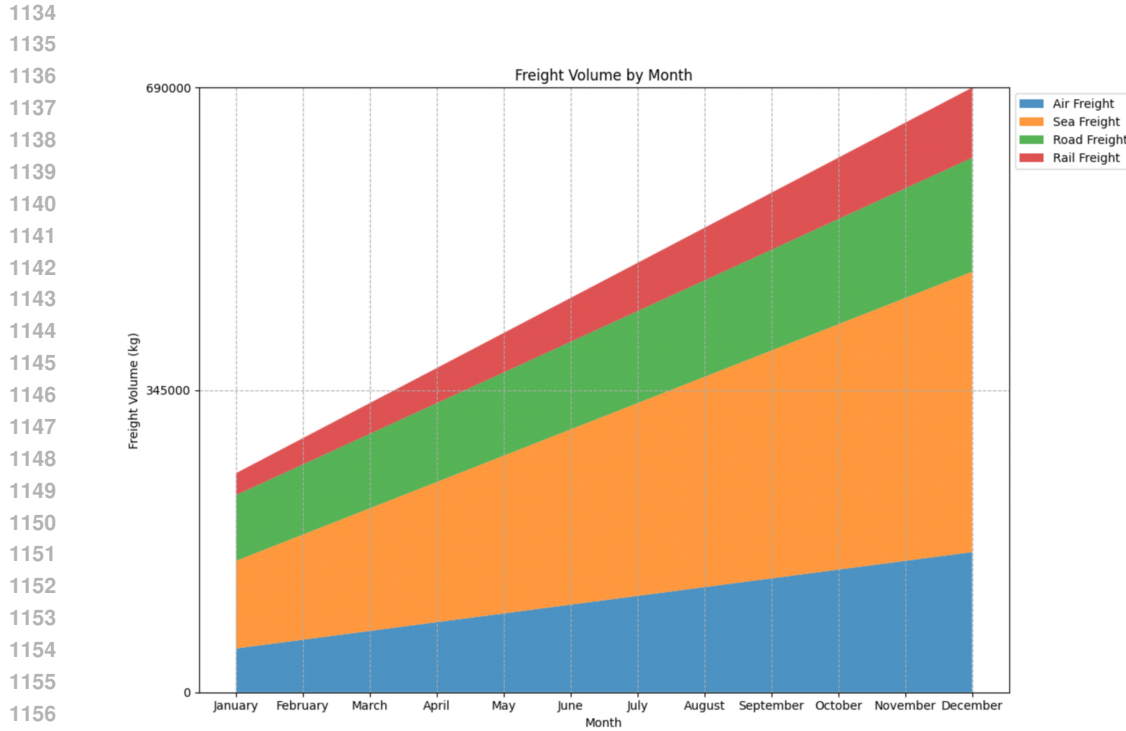
1111     **Towards Dynamic Strategy Composition.** Looking further ahead, our current framework makes  
 1112     a discrete selection between predefined strategies. A significant extension would be for future  
 1113     systems to dynamically *compose* novel strategies from a set of primitive cognitive operations. For  
 1114     instance, when analyzing a complex visualization, an advanced system might synthesize a hybrid  
 1115     approach on the fly: invoking its internal graph-based logic for structural analysis while using its  
 1116     time-series forecasting logic for temporal patterns. This compositional flexibility, guided by a learned  
 1117     meta-policy, would represent a significant leap towards more human-like adaptability.

1118     **The Path Forward.** The journey from narrow tools to general intelligence will likely require  
 1119     architectural innovations that foster cognitive flexibility. Our adaptive framework, though applied to  
 1120     chart understanding, provides a concrete instantiation of these principles. By teaching a model to  
 1121     recognize when formal reasoning is a powerful asset versus a brittle liability, we take a tangible step  
 1122     toward systems that reason not just powerfully, but appropriately. The ultimate goal is not to build  
 1123     models that always default to their most complex methods, but ones that can gracefully match their  
 1124     computational effort and reasoning style to the structure of the problem at hand—a hallmark of true  
 1125     intelligence.

## 1127     I DETAILED CASE STUDIES

1129     This section provides the full visualizations and detailed model outputs for the qualitative analysis.  
 1130     Each case includes the figure, the task details, and the verbatim model outputs from both a baseline  
 1131     and our adaptive model.

1132



[Question] How much did the sea freight volume increase from January to December?

[ground\_truth] 220000 kg

[CoT]  
 To determine the increase in sea freight volume from January to December, we need to follow these steps:  
 1. Identify the sea freight volume in January.  
 2. Identify the sea freight volume in December.  
 3. Subtract the January volume from the December volume to find the increase.  
 Let's start by estimating the sea freight volumes for January and December from the stacked area chart:  
 In January, the sea freight volume appears to be around 100,000 kg.  
 In December, the sea freight volume appears to be around 250,000 kg.  
 Now, we calculate the increase:  

$$\text{Increase} = \text{December volume} - \text{January volume} = 250,000 \text{ kg} - 100,000 \text{ kg} = 150,000 \text{ kg}$$
  
 Thus, the increase in sea freight volume from January to December is  

$$\boxed{150000}.$$

[Adaptive(ours)]  
<CODE>  
First, let's reconstruct the chart data into a pandas DataFrame for analysis:  

$$\text{python}\n\text{import pandas as pd}\n\text{data} = \{\text{'Month': ['January', 'February', 'March', 'April', 'May', 'June', 'July', 'August', 'September', 'October', 'November', 'December'], 'Air Freight': [100000, 120000, 140000, 160000, 180000, 200000, 220000, 240000, 260000, 280000, 300000, 320000], 'Sea Freight': [150000, 170000, 190000, 210000, 230000, 250000, 270000, 290000, 310000, 330000, 350000, 370000], 'Road Freight': [70000, 80000, 90000, 100000, 110000, 120000, 130000, 140000, 150000, 160000, 170000, 180000], 'Rail Freight': [20000, 25000, 30000, 35000, 40000, 45000, 50000, 55000, 60000, 65000, 70000, 75000]},\n\text{chart\_data} = \text{pd.DataFrame(data)}$$
  
Now, we will analyze the sea freight volume increase from January to December.  

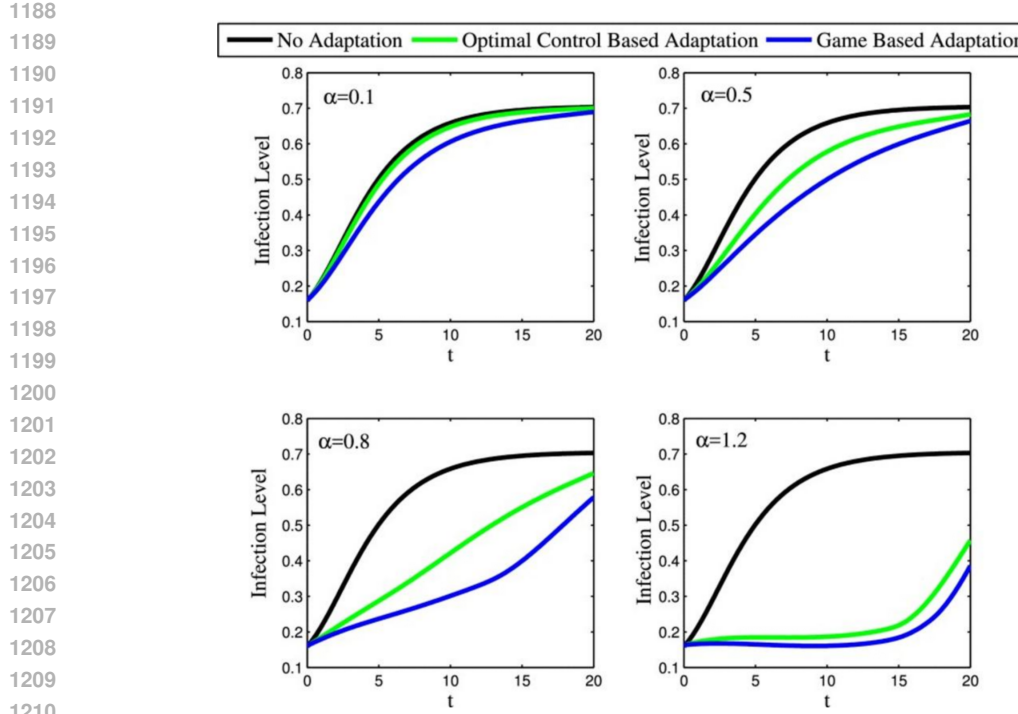
$$\text{Sea Freight in January} = 150000 \text{ kg}$$
  

$$\text{Sea Freight in December} = 370000 \text{ kg}$$
  
The increase in sea freight volume from January to December is:  

$$\text{increase} = \text{chart\_data}[\text{'Month'} == \text{'December'}, \text{'Sea Freight'}].values[0] - \text{chart\_data}[\text{'Month'} == \text{'January'}, \text{'Sea Freight'}].values[0]$$
  

$$\text{increase} = 370000 - 150000 = 220000 \text{ kg}$$

**Figure 8:** Case Study 1: High-Programmability Chart from ChartX. On a standard stacked area chart from ChartX that required precise calculation, our adaptive model correctly chose the <CODE> path, extracting exact data and computing the correct answer. In contrast, a fixed ‘Standard CoT’ model relied on visual estimation and failed. This shows the model’s ability to leverage code for precision.



[Question] What is the value of the  $\alpha$  of the subplot where the Optimal Control Based Adaptation and Game Based Adaptation has most difference in Infection Level at  $t = 15$ ?

[ground\_truth] 0.8

[Code-CoT]

First, let's create a DataFrame `chart\_data` with the necessary data:  
`python\nimport pandas as pd\n\nchart_data = pd.DataFrame({\n 'alpha': [0.1, 0.5, 0.8, 1.2],\n 'no_adaptation': [0.7, 0.7, 0.7, 0.7],\n 'optimal_control': [0.7, 0.7, 0.65, 0.45],\n 'game_based': [0.7, 0.65, 0.55, 0.4]\n})\n\nNow, let's plot the data using Matplotlib. Here is the code to create the plot:  
python\nimport matplotlib.pyplot as plt\n\nfig, axs = plt.subplots(2, 2, figsize=(10, 8))\nfor ax, alpha, no_adaptation,\noptimal_control, game_based in zip(axs.flatten(), chart_data['alpha'], chart_data['no_adaptation'],\nchart_data['optimal_control'], chart_data['game_based']):\n ax.plot(chart_data['t'], no_adaptation,\n label='No Adaptation', color='black')\n ax.plot(chart_data['t'], optimal_control,\n label='Optimal Control Based Adaptation', color='green')\n ax.plot(chart_data['t'], game_based,\n label='Game Based Adaptation', color='blue')\n ax.set_xlabel('t')\n ax.set_ylabel('Infection Level')\n ax.set_title(f'\u03b1={alpha}')\n ax.set_xlim(0, 20)\n ax.set_ylim(0.1, 0.8)\n ax.legend()\nplt.show()`

Now, to answer the question: We need to find the value of  $\alpha$  where the difference between Optimal Control Based Adaptation and Game Based Adaptation is the most significant at  $t = 15$ . From the plots:  
- At  $\alpha = 0.1$ , the difference is minimal.  
- At  $\alpha = 0.5$ , the difference is moderate.  
- At  $\alpha = 0.8$ , the difference is significant.  
**At  $\alpha = 1.2$ , the difference is the most significant.**  
Thus, the value of  $\alpha$  where the difference is the most significant at  $t = 15$  is:

[Adaptive(ours)]

The question asks for the value of  $\alpha$  where the difference between Optimal Control Based Adaptation and Game Based Adaptation is most significant at  $t = 15$ . From the visual inspection of the subplots, it appears that this difference is most pronounced in the subplot where  $\alpha = 0.8$ .  
**<DIRECT>**  
At  $t = 15$ , the infection level for  $\alpha = 0.8$  is significantly different between the Optimal Control Based Adaptation (green line) and the Game Based Adaptation (blue line). The green line (Optimal Control Based Adaptation) is higher than the blue line (Game Based Adaptation) at this point.

**Figure 9:** Case Study 2: Low-Programmability Chart from CharXiv. Faced with a complex scientific plot from CharXiv requiring qualitative comparison, a fixed code-based model failed by hallucinating a data table. Our adaptive model, however, correctly identified the task's low programmability and chose the **<DIRECT>** path. It performed a robust visual comparison, leading to the correct answer and demonstrating its critical skill in avoiding tools when they are unsuitable.

1242 **J IMPLEMENTATION AND HYPERPARAMETER DETAILS**  
12431244 Our model was trained using the configuration and hyperparameters summarized in Table 9. We  
1245 used the EasyRL Zheng et al. (2025) framework for our reinforcement learning implementation. The  
1246 base model, Qwen2.5-VL-7B, was trained for 200 episodes. The vision tower of the model remained  
1247 frozen during training to preserve its pre-trained perceptual capabilities.  
12481249 **Table 9:** Training Configuration Details

1250 <b>Configuration</b>	1251 <b>Value</b>
<i>1252 <b>Model Configuration</b></i>	
1253 Base Model	Qwen2.5-VL-7B
1254 Vision Tower	Frozen
1255 Precision	BFloat16
1256 Max Prompt Length	5,120 tokens
1257 Max Response Length	3,072 tokens
<i>1258 <b>Data Configuration</b></i>	
1259 Seed	42
1260 Shuffle	True
1261 Filter Overlong Prompts	True
<i>1262 <b>Training Hyperparameters</b></i>	
1263 Algorithm	GRPO (without KL penalty)
1264 Learning Rate	$1.0 \times 10^{-6}$
1265 Optimizer	AdamW (BF16 variant)
1266 Global Batch Size	64
1267 Rollout Batch Size	256
1268 Micro Batch Size (Update)	4
1269 Micro Batch Size (Experience)	16
1270 Training Episodes	4
1271 Gradient Clipping	1.0
<i>1272 <b>Rollout Configuration</b></i>	
1273 Number of Rollouts ( $n$ )	5
1274 Temperature	1.0
1275 Top-p	0.99
<i>1276 <b>Infrastructure</b></i>	
1277 GPUs	8 × NVIDIA H800
1278 Tensor Parallelism	1
1279 FSDP	Enabled
1280 CPU Offloading	Disabled
1281 Gradient Checkpointing	Enabled
<i>1282 <b>Validation</b></i>	
1283 Validation Batch Size	512
1284 Validation Frequency	Every 5 episodes
1285 Validation before Training	Yes

1286  
1287  
1288  
1289  
1290  
1291  
1292  
1293  
1294  
1295